Desalination and Water Treatment
www.deswater.com

doi: 10.5004/dwt.2018.22129

105 (2018) 51–61
February

Antimicrobial and pressure resistant polysulfone blended ultrafiltration membranes with core-shell ZnO microspheres

Zehai Xu[a,b,†], Ling Wang[b,c,†], Zhen Xue[b], Wentao Xu[a], Xinyan Wang[d], Guoliang Zhang[a,b,*]

[a]*College of Chemical Engineering and Material Science, Quanzhou Normal University, Quanzhou 362000, China, Tel./Fax 86-571-88320863, email: guoliangz@zjut.edu.cn*
[b]*Institute of Oceanic and Environmental Chemical Engineering, State Key Lab Breeding Base of Green Chemical Synthesis Technology, Zhejiang University of Technology, Hangzhou 310014, China*
[c]*Hangzhou Special Equipment Inspection and Research Institute, Hangzhou, 310051, China*
[d]*Shandong Zhaojin Motian Co.,Ltd, Zhaoyuan 265400, China*

Received 14 February 2017; Accepted 2 February 2018

ABSTRACT

Hybrid membranes prepared by blending antibacterial nanoparticles and organic materials are fascinating for creating novel filtration materials with improved properties such as excellent antimicrobial activity, good permeability and mechanical properties. In this study, composite zinc oxide microspheres with elaborate hollow structures were constructed as multi barrier layers for both effective release control and pressure resistance. Different polysulfone (PSF) membranes with competitive antimicrobial properties toward Staphylococcus aureus and *Escherichia coli* were synthesized by applying, single-shell ZnO microspheres (S membranes), core-shell ZnO microspheres (C1 membranes) and levodopa (dopa) coated core-shell ZnO microspheres (C2 membranes) via phase inversion with ZnO nanoparticles (Z membranes) for comparison. Since the rate of zinc ions diffusion can be limited due to the barriers created by the multi shells of hollow microspheres and adhesion layer with catechol and indole functional groups, the prepared polysulfone ultrafiltration membranes can keep good balance between structure and antimicrobial feature. In the filtration process, the novel blended membranes exhibited fascinating pure water flux at least two times higher than that of pure PSF membrane, and the rejection rate for BSA reached 91.2%. After two cycles of operation, they displayed excellent anti-fouling ability as well as long-term stability with little leakage of zinc ions. Moreover, as multi-layer structure can obviously improve the mechanical strength of colloids, the prepared membranes exhibited attractive pressure resistant ability which may effectively withstand harsh conditions in the practical pressure-driven process.

Keywords: Polysulfone blended ultrafiltration membranes; Zinc oxide microspheres; Core-shell structure; Antimicrobial; Pressure resistant

1. Introduction

Polysulfone (PSF), as one of the most promising membrane materials, has attracted expanding interests for its prominent properties and application in various fields such as chemical separation, food, biomedical and environmental fields [1–3]. However, most of prepared PSF membranes are inherently hydrophobic, which increases their resistance to water permeation and energy consumption during membrane filtration process [4,5]. Moreover, some microorganisms are easily induced on the surface of membrane to cause biofouling. The growth of biofilms can reduce the membrane flux and enhance the operational charges to a large extent [6,7]. Therefore, the rational design and synthesis of antimicrobial membranes with high activity and long-term stability has been focused in recent years.

*Corresponding author.

†These authors contributed equally.

To address these challenges, varieties of methods, including surface grafting, physical modification and coating have been broadly used to fabricate antimicrobial membranes [8–10]. Among them, physical modification by blending antibacterial nanomaterials such as Cu_2O, TiO_2, SiO_2, Ag, ZnO, polycations and chitosan into membranes has been conducted as a smart strategy to increase the antimicrobial activity of membranes [7,11–14]. In particular, semiconductor zinc oxide nanomaterials have been widely concerned in terms of the unique properties, especially their bactericidal activity. Some researches found that they exhibited broad spectrum antibacterial behavior against a series of Gram-positive and Gram-negative bacteria, and also showed bactericidal activity toward spores and fungal pathogens in high pressure and high temperature conditions [15,16]. Reports have also indicated that zinc oxide nanoparticles may generate reactive oxygen species (ROS), interact with protein and DNA and damage cell membrane permeability [17]. Therefore, immobilization of zinc oxide nanomaterials into the membranes appears to be a great choice for surface antibacterial treatment. Several studies have confirmed this action in assembling zinc oxide nanoparticles into polyethersulfone/aminated polyethersulfone ultrafiltration membranes and in decorating polyamid thin film composite PA(TFC) membrane with ZnO nanoparticles [18,19]. Despite the progress achieved so far, there are still big challenges for the nanoparticles blended membranes, for example, the leakage of zinc ions and the crushing problems under high pressures. Because ZnO nanoparticles are difficult to be fixed in polymers firmly by physical blending, the release of metal ions from the membrane would seriously reduce the antibacterial activity and lead to secondary pollution. As for this challenge, one effective strategy is the combination of antibacterial nanoparticles and polymer colloids since the adhesion of nanoparticles on polymer colloids can effectively keep antibacterial activity and restrain the leakage. Another strategy may be the rational design of a novel membrane which takes advantage of some smart structured nanomaterials like nanowires, nanotubes and hollow microspheres [20]. As the core-shell avermectin microspheres has been reported to exhibit a reduction in the initial release as compared to the nanoparticles [21], we go forward to think it a feasible strategy to prepare ZnO-organic antimicrobial membranes with controlled release by employing core-shell ZnO microspheres as robust nanofillers. As we know, so far there is no report focusing on polymeric membrane blended with core-shell ZnO hollow microspheres to achieve desirable antimicrobial activity with necessary stability and sustained release property.

In this study, by blending different kinds of core-shell ZnO microspheres, novel hybrid polysulfone ultrafiltration membranes with superior antibacterial activity and pressure resistant property were successfully developed via a phase inversion method (Fig. 1). Besides the structure barriers rising from ZnO hollow microspheres, levodopa layer was further applied to cover on the surface of microspheres to further prevent the release of metal ions. In the meantime, the compatibility of membranes can be greatly enhanced due to large number of functional groups in the colloids. Compared with the weak pressure resistance presented in existing membranes, here the improved structure composed of multi-shells of hollow microspheres and adhesion layer with catechol and indole functional groups can greatly reinforce the mechanical strength of novel porous membranes.

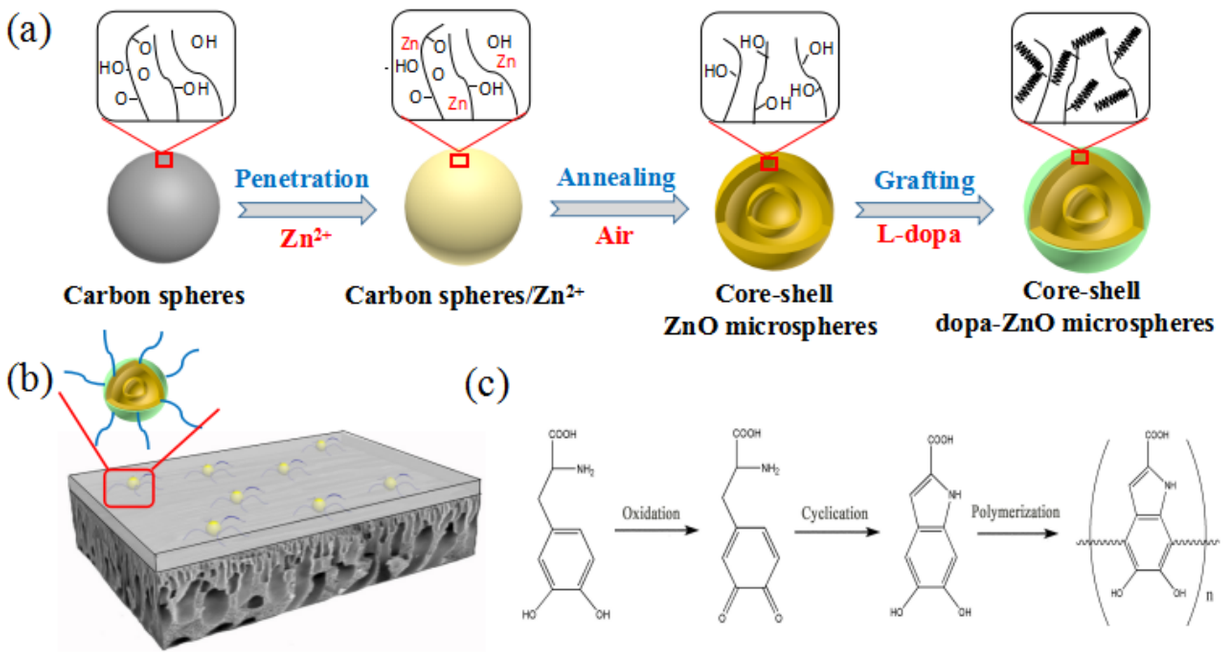

Fig. 1. Scheme of synthesis procedure of core-shell dopa-ZnO microspheres (a), prepared blended membranes (b), and possible mechanism for levodopa ploymerization (c).

2. Experimental

2.1. Materials

PSF (MW 65,000) was supplied by Shuguang Chemical Company (Shanghai, China). N, N-dimethylacetamide (DMAc) with reagent grade was severed as solvent and provided from Sinopharm Chemical Reagent Co. (Shanghai, China). The other chemicals including zinc nitrate, levodopa (dopa), sucrose and ethyl alcohol were all of AR grade. Deionized water was prepared by a electro-deionization system. The ion concentration of deionized water was monitored by a Metrohm 861 Compact IC and an IRIS Intrepid ICP.

2.2. Synthesis of core-shell ZnO and dopa-ZnO microspheres

ZnO microspheres were fabricated via a facile template method. A hydrothermal process with the emulsion polymerization reaction of sugar was employed for the fabrication of carbonaceous microspheres [22]. Then 0.6 g prepared carbonaceous microspheres were spred around in zinc nitrate solution (20 mL, 3 M). After 15 min of ultrasonic treatment, the prepared suspension was aged for 6 h at 25°C and then centrifuged and dried in an oven at 80°C over night. Core-shell ZnO microspheres were obtained by directly calcining in air at 500°C with the rate of 1°C min^{-1}. As for single-shell ZnO hollow microspheres and ZnO nanoparticles, the difference was the heat treatment. The single-shell ZnO hollow microspheres and ZnO nanoparticles were obtained by calcining in air at 460°C with the rate of 2°C min^{-1} and at 440°C with the rate of 5°C min^{-1}, respectively. In order to improve the compatibility of blended membranes, the core-shell ZnO microspheres were further covered with levodopa and labelled as core-shell dopa-ZnO spheres. The size of all microspheres and nanoparticles were controlled at a similar level.

2.3. Characterization of ZnO microspheres

X-ray diffraction patterns (XRD) measurements were operated with X'Pert PRO X-ray diffractometer in the range from 20° to 80°. The formation of covalent bonds in this reaction can be observed by Fourier transform infrared spectroscopy (FTIR, Nicolet 6700, USA). The ZnO microspheres were also determined by scanning electron microscope (SEM, TM1000, Japan) and transmission electron microscopy (TEM, JEM-1200EX, Japan) and energy dispersive X-ray spectroscopy (EDX) analysis.

2.4. Membrane preparation

PSF blended membranes with pure core-shell ZnO microspheres (C1 membranes): core-shell ZnO microspheres (0, 0.1, 0.3, 0.5 and 1.0 wt.%, respectively) were dissolved into N,N-dimethylacetamide and the mixture was treated with ultrasonic treatment for 0.5 h, then PSF (15.0–16.0 wt.%) was put in the mixture and dissolved into it. The casting solution was treated with constant stirring for 24 h and ultrasonicated 30 min for degassing. Afterwards, the dope solution was extended on a glass plate and casted by employing a casting knife with 200 μm thickness. The glass plate was then put in water bath for phase inversion. After the phase separation and membrane formation, the membrane samples were eventually rinsed with deionized water and stored in it. PSF blended membranes with core-shell dopa-ZnO microspheres (C2 membranes), single-shell ZnO microspheres/PSF (S membranes) and ZnO nanoparticles/PSF blended membranes (Z membranes) were synthesized with same method mentioned above.

2.5. Membrane characterizations

For the morphological characterization for surface and cross-section of membranes, SEM analysis was carried out. As for cross section measurement, the membranes were initially fractured by liquid nitrogen.

To investigate the hydrophilicity of prepared membranes, water contact angle measurement was directly taken by using a contactangle goniometer (Dataphysics OCA20, Germany). The average value of contact angle was obtained by calculating the results from five tests.

The mechanical properties of membrane samples were determined by uniaxial tension testing equiped with an INSTRON5966 electronic universal testing machine at room temperature. Membrane samples were sheared into a rectangle (10×50 mm^2). For each sample, three experimental tests were measured and the average value was calculated.

2.6. Antibacterial activity tests

The prepared samples for pure PSF, Z membranes, S membranes, C1 membranes and C2 membranes were used for evaluating the antibacterial activity against *S. aureus* bacteria (100 μL of 10^6 cells/ml) by zone of inhibition (mm). All membranes were disinfected by autoclaving for half an hour prior to test. Then membranes with 8.0 mm in diameter were put on *S. aureus* bacteria Luria-Bertani (LB) agar plates and incubated at 37°C for 15 h. After that, the bacteria colonies can be visually observed in the agar plates. In order to further estimate the bactericidal activity, the pure and blended PSF membranes were immersed separately into the liquid medium (10 ml of 10^6 cells/ml) for a period of 4 d. Several pieces of the prepared membrane samples were taken out from the shaking incubator at different time intervals. To further observe the differences in surface morphology, the membranes were treated with a modified method in which the adhered bacteria were fixed on the surface of each membrane sample by soaking into glutaraldehyde solution.

2.7. Zinc ions leaching test

The stability of the ZnO nanomaterials blended in the membranes was investigated by the leaching test. The membrane samples were sheared into cycles with 8 mm in diameter, and then several samples with same quality were soaked into 30 ml deionized water. The total concentrations of zinc ions were first controlled at same level and monitored after nitrification. After a set time, the content of zinc ions in suspending liquids obtained every time was dissolved by nitric acid prior to the detection by atomic absorption spectrometer.

In order to further investigate the release of zinc ions from prepared membranes, filtration test was carried out. 1 L deionized water was filtrated with the blended membranes (7.065 cm^2) at 0.1 MPa for 15 h. The content of zinc ions in the permeate samples were characterized by atomic absorption spectrometer.

2.8. Separation performance of membranes

Water permeability of fabricated membranes was investigated through cross flow filtration experimental equipment. Membrane samples were cut into a cycle (7.065 cm^2). After pressurized at 0.2 MPa for 30 min first, the membranes were fed with deionized water at 0.1 MPa for about 1 h. In order to obtain the accurate values of pure water flux and BSA rejection rate for prepared hybrid membranes, five independent samples were measured at least and the average value was calculated. The pure water flux is defined as below:

$$PWF = \frac{Q}{A \times t} \tag{1}$$

where PWF is pure water flux (L m^{-2} h^{-1}), Q is quantity of permeate (L), t is permeation time (h) and A is effective membrane area (m^2).

BSA solution (0.2 g/L) was prepared by using 10 mM phosphate buffered saline (PBS) as solvent. UV-vis spectrophotometer was applied to evaluate the protein content of the feed (C_f) and the permeate (C_p). The formula of BSA rejection ratio R_{BSA} (%) is as follows:

$$R_{BSA}(\%) = \left(1 - \frac{C_p}{C_f}\right) \times 100 \tag{2}$$

The porosity of membranes was calculated after removing the water droplets from the membrane. The membrane mean pore radius r_m (nm) was also evaluated by Guerout-Elford-Ferry formula [23]. The porosity ε (%) is defined as follows:

$$\varepsilon(\%) = \frac{W_w - W_d}{\rho_w \times A \times \delta} \tag{3}$$

where W_w (g) and W_d (g) are the weights of the wet membranes and the dry membranes, respectively. ρ_w is the density of water (g cm^{-3}); A is the area of membrane (cm^2); δ is the membrane thickness (cm).

3. Results and discussions

3.1. Morphology and structure of core-shell ZnO microspheres

In order to evaluate the morphology of core-shell ZnO hollow microspheres, SEM and TEM analysis were carried out. Fig. 2a exhibits SEM image of core-shell ZnO hollow microspheres which have similar shape and size. The surfaces of all spheres are relative smooth and the size distributions are in the range of 500–800 nm for these hollow microspheres. Moreover, the image of split hollow sphere (inset of Fig. 2a) provides the evidence of existence of the hollow structure. Fig. 2b shows the TEM image of prepared micropsheres with a double-shell structure clearly. The image of high-resolution lattice fringes (Fig. 2c) reveals a lattice distance of 0.19 nm, corresponding to (102) plane of ZnO phase. Moreover, fast Fourier transformation (FFT) pattern also confirms the phase of fabricated hollow spheres as zinc oxide. Element map (Fig. 2d) predicts that only C, O and Zn elements are detected, no impurities are observed in the samples. The XRD patterns of the fabricated core-shell ZnO and dopa-ZnO microspheres exhibit a typical phase of zincite ZnO (JCPDS No:36-1451) and all peak positions can be identified to reference data [24–26]. In order to identify the existence of poly (levodopa), FTIR analysis was carried out. Two new peaks appear at 1491 cm^{-1} and 1259 cm^{-1} in FTIR spectrum, which can be assigned to N-H scissoring and C-O stretching, respectively. Moreover, a new band appears at 1594 cm^{-1} (phenylic C=C stretching and superposition of N-H bending), all new bands reflect that adhesion layer formed by self-polymerization levodopa provide lots of chemical adsorption sites.

3.2. Mechanical strength

The effects of core-shell ZnO microspheres addition on mechanical strength of fabricated membranes were evaluated by uniaxial tension test. As shown in Fig. 3 and Table 1, the tensile strength and elongation ratio of all blended membranes were increased with the ZnO addition. In particular, higher percentage elongation and tensile strength were achieved with enhancing fillers concentration from 0.1 wt% to 0.5 wt%. However, when the addition amount was 1.0 wt%, although the value of tensile strength reached up to 4.63 MPa, the elongation ratio had a certain degree of decrease. This phenomenon was similar to the previous report, when the content of ZnO microspheres reached 1.0 wt%, the aggregation of ZnO microspheres would cause the reduction of compressive strength, and consequently reduce the elongation ratio [27]. Therefore, ZnO microspheres blended membranes with superior mechanical properties can be rationally controlled through employing an appropriate content of fillers, which can be applied under high pressure environment.

3.3. Morphology of membrane samples

From the cross-section morphologies of pure PSF, C1 and C2 membranes were depicted in Fig. 4. Observable porous and finger-like structure can be found on top surface in all membranes. After being modified with ZnO microspheres, more finger-like pores became wider and appeared in the blended membranes. This phenomenon is similar to previous reports that the increase of suspension viscosity was induced by adding inorganic nanomaterials, which led microspheres to move hardly during the phase inversion process [7,28,29]. Furthermore, more dense pores were formed after coating ZnO microspheres with poly (levodopa). It is beneficial to generate more small pores

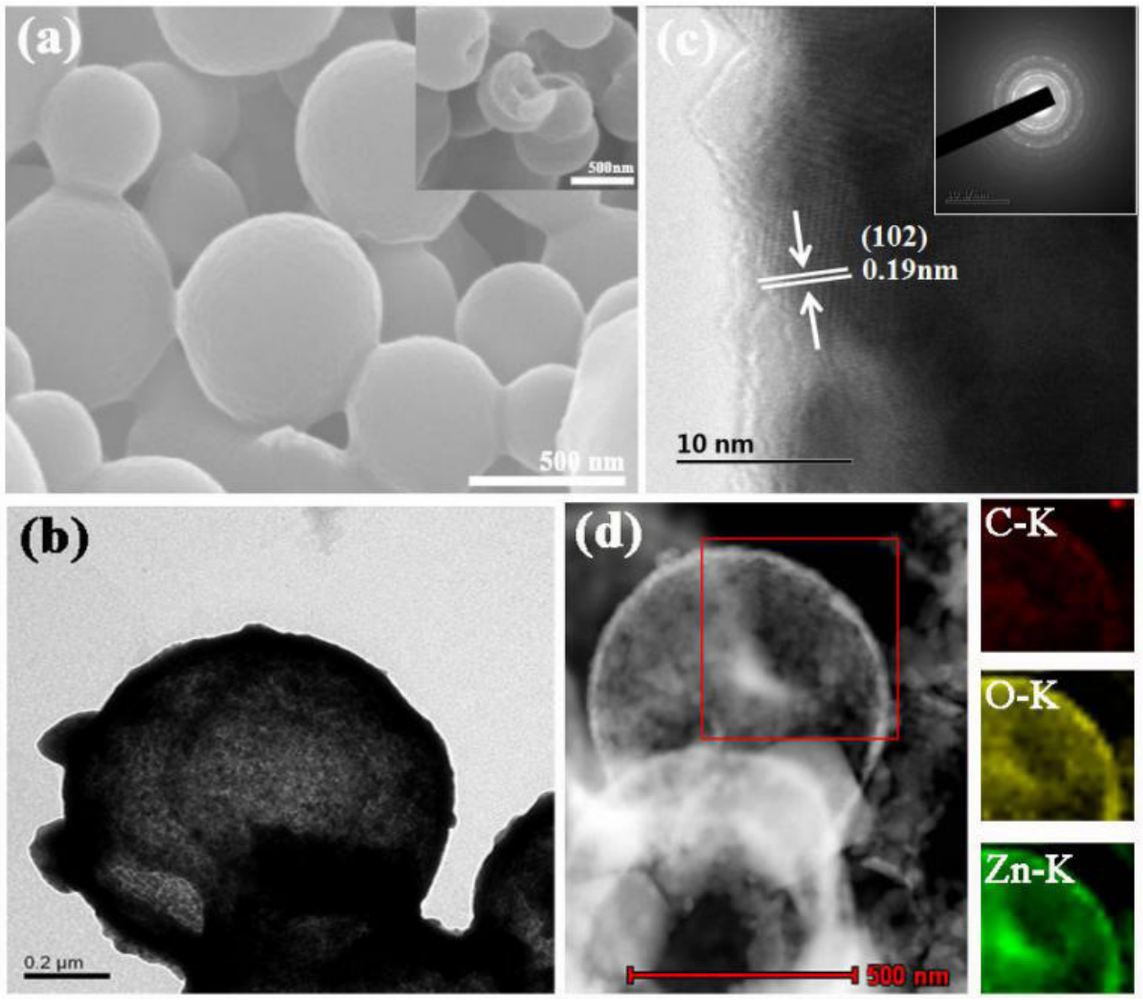

Fig. 2. SEM images of prepared core-shell ZnO microspheres (a) and split spheres (inserted graph), TEM and HRTEM images (b, c) of core-shell ZnO microspheres, the inset image is corresponding fast-Fourier-transform (FFT) pattern, element map of the core-shell ZnO microspheres (d).

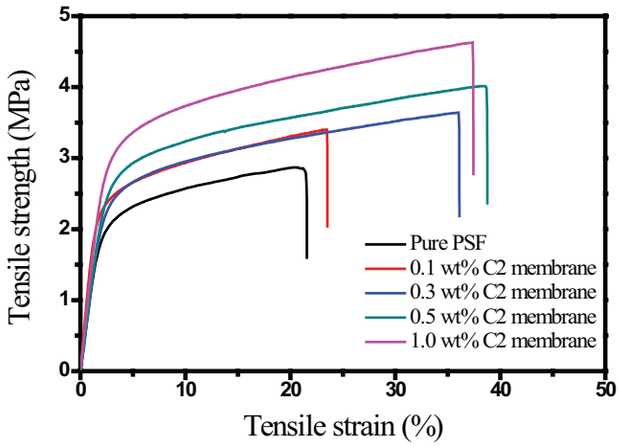

Fig. 3. Strength-strain curves of the pure PSF and C2 blended membranes.

Table 1
Mechanical properties of blended membranes

Sample	Tensile strength (Mpa)	Tensile strain (%)
Pure PSF	2.85 (±0.1)	21.58 (±1.8)
0.1 wt% C2 membranes	3.64 (±0.15)	23.53 (±2.6)
0.3 wt% C2 membranes	4.12 (±0.08)	36.10 (±3.1)
0.5 wt% C2 membranes	4.85 (±0.11)	38.76 (±2.2)
1.0 wt% C2 membranes	5.08 (±0.09)	37.43 (±1.9)

which can prevent big molecules during filtration process. The surface morphologies of pure PSF and as-prepared blended membranes (Fig. 4d and 4f) after introduction of core-shell ZnO and dopa-ZnO microspheres are smooth without any cracks.

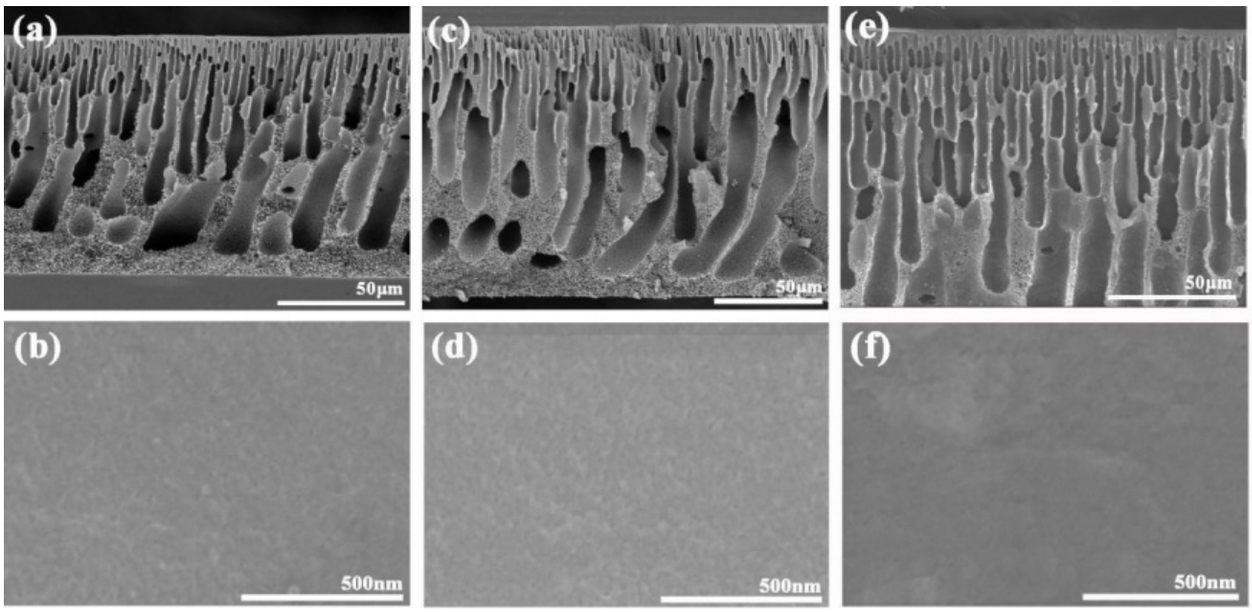

Fig. 4. Cross section and surface SEM images of PSF (a, b), C1 membranes with 1.0 wt% filler contents (c, d) and C2 membranes (e, f).

Table 2
Porosity, mean pore size and contact angle of the blended membranes.

Sample	Porosity (%)	Mean pore size (nm)	Contact angle (°)
Pure PSF	68.5 (±2.6)	14.5 (±0.5)	91.4 (±1.5)
0.1 wt% C2 membranes	72.5 (±2.9)	31.7 (±0.7)	88.3 (±2.2)
0.3 wt% C2 membranes	76.4 (±2.8)	34.5 (±0.7)	82.4 (±1.7)
0.5 wt% C2 membranes	74.9 (±3.1)	32.5 (±0.6)	78.3 (±2.3)
1.0 wt% C2 membranes	71.8 (±3.4)	29.2 (±0.8)	73.1 (±1.9)

3.4. Permeation property

The separation behavior of fabricated blended membranes was evaluated by ultrafiltration tests. Before BSA filtration experiments, the pure water flux of membranes was investigated. Water permeability increased with the addition of different ZnO hollow microspheres. The pure water flux of C1 membrane was 108.0, 139.6, 88.9, 83.8 L m^{-2} h^{-1} when the concentration of blended core-shell ZnO hollow microspheres was 0.1, 0.3, 0.5 and 1.0 wt%, respectively. It is clear that the presence of ZnO hollow microspheres in the membranes effectively enhanced the water permeability. Furthermore, more hydrophilicity was achieved with the addition of nanofillers, this was confirmed by contact angle analysis (Table 2). However, an increase in the proportion of nanofillers in the membrane may lead the pore blockage and reduction of pure water flux [30,31]. The protein rejection was investigated with filtration test by employing BSA aqueous solution. As depicted in Fig. 5a, both C1 and C2 membranes with core-shell ZnO microspheres exhibited an obvious increment of pure water flux compared to pure PSF membrane, in which the permeate flux of C2 membrane

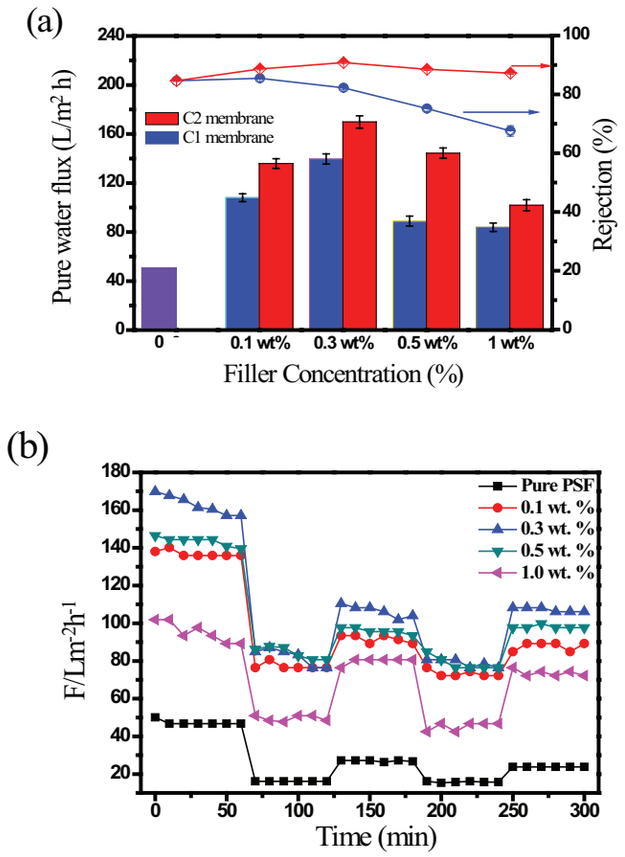

Fig. 5. Pure water flux and BSA rejection of C1 membranes and C2 membranes with different filler concentrations (a), water flux recovery of C2 membranes after two cycles of BSA solution (b).

was about 10% higher than that of C1 membrane. For the BSA rejection, the rejection rate of C2 membrane was above 91% when addition amount was 0.3 wt%. Since levodopa can be easily attached on the surface of ZnO spheres with self-polymerization, the compatibility and hydrophilicity of membranes can be enhanced due to catechol and indole functional groups [32,33]. The result is in agreement with the SEM analysis (Fig. 4). Moreover, the reusability and stability of prepared membranes were demonstrated in Fig. 5b, two cycles with BSA solution were performed (three water filtrations: 0–60, 120–180 and 240–300 min and two BSA filtrations: 60–120 and 180–240 min). The excellent anti-fouling performance of fabricated membranes was reflected by the high flux recovery over two cycles of BSA solution.

3.5. Antibacterial activity

To verify the antimicrobial behavior of prepared blended membranes, inhibition zone tests were carried out to assess their antimicrobial activities. ZnO nanoparticles, single-shell and core-shell ZnO and dopa-ZnO microspheres with amount of 1.0 wt% were added into the membranes. The results of the inhibition zone method against *Staphylococcus aureus* (abbreviated as *S. aureus*) were shown in Fig. 6. The pure PSF membrane was used as a negative control, the others blended membranes were set as positive control. As expected, no visible zones were detected in the plate of pure PSF membrane. This implied that *S. aureu*s was deactivated by the antimicrobial ZnO nanomaterials emigrated from the membranes. The radial diameters of the inhibiting zones for Z membranes, S membranes, C1 membranes and C2 membranes were 11.2, 10.3, 8.9 and 8.6 mm, respectively. The results indicated that less zinc ions release from C1 and C2 membranes compared to the other blended membranes, which is in agreement with our assumption mentioned above. Moreover, shaking flask method was also employed to investigate the viability toward Escherichia coli (abbreviated as *E. coli*) and *S. aureus*. As depicted in Fig. 7, numerous bacteria grew finely on the pure PSF membrane, while almost no bacteria can be observed on C1 and C2 membranes. This can be attributed to that a great number of bacteria were unable to be adhered to the surface of membranes and a spot of bacteria attached to the membranes were killed by zinc ions. The result is in agreement with previous literature that ZnO nanomaterials can restrain the growth of *E. coli* and *S. Aureus* [35–37].

3.5. Leaching test

Zinc oxide nanomaterials with bactericidal activity blended into membranes can weaken membrane biofouling through releasing zinc ions. However, the leakage of zinc ions would limit the practical application. Therefore, in order to obtain a long-lasting bactericidal duration, the leaching rate of zinc ions from the blended membranes should be rationally controlled. It is meaningful to investigate the stability difference for ZnO nanoparticles, single-shell, core-shell ZnO and dopa-ZnO microspheres blended in the membranes.

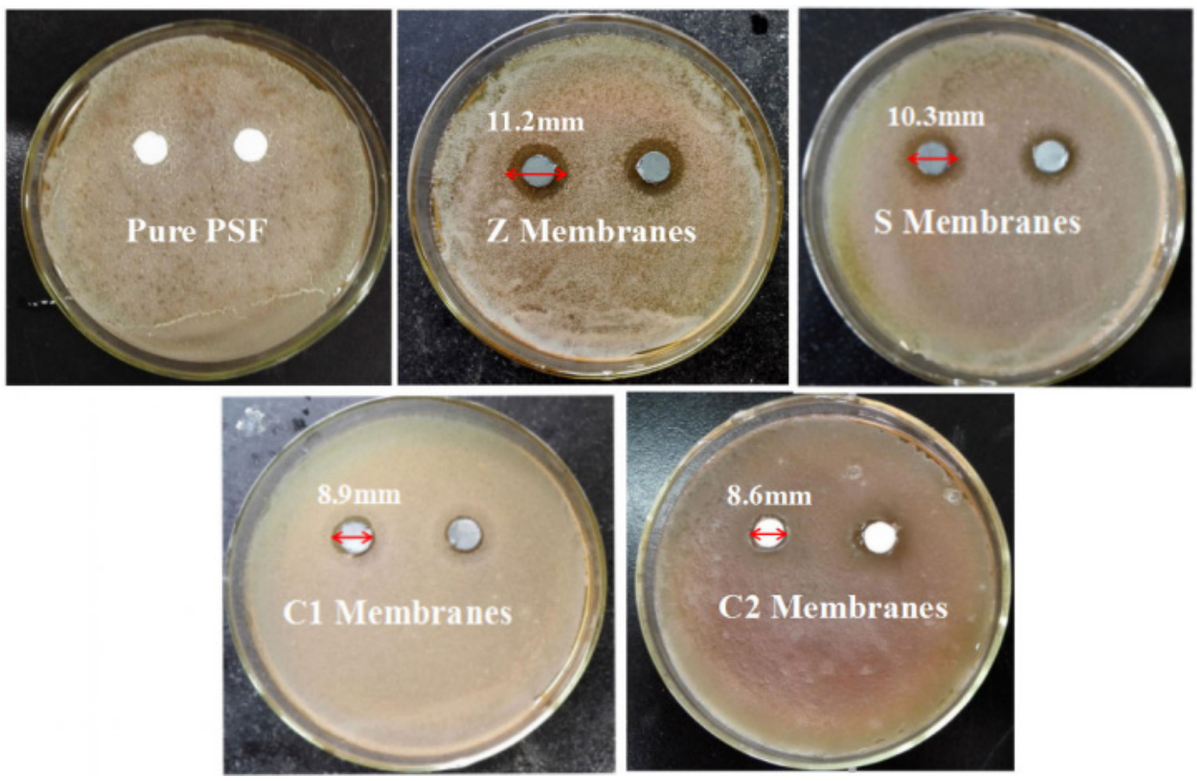

Fig. 6. Inhibition zone of membranes with *S. Aureus*.

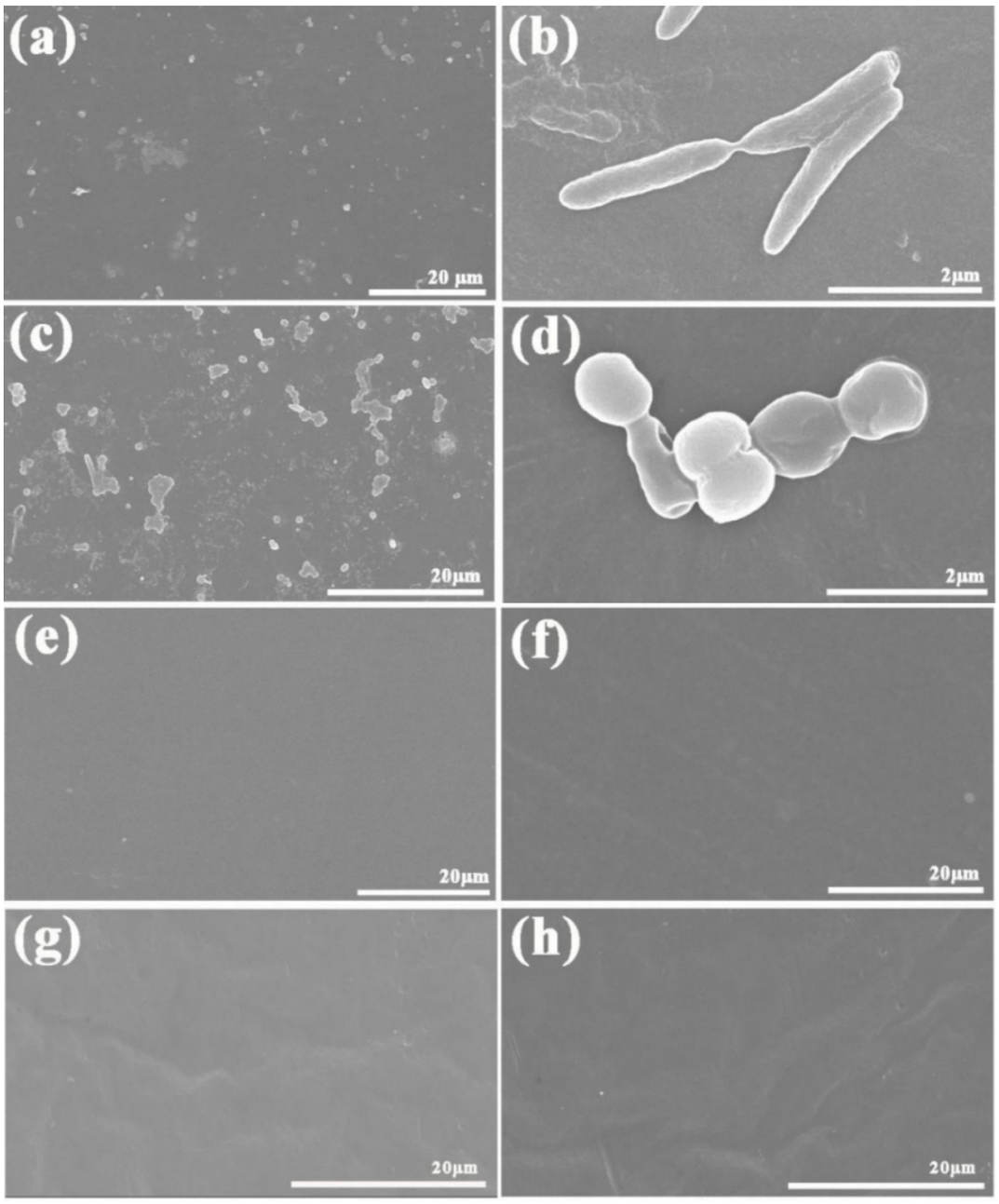

Fig. 7. SEM images showing bacterial adhesion and growth on the pure PSF membrane (*E. coli* (a, b) and *S. aureus* (c, d)), C1 membranes (*E. coli* (e) and *S. Aureus* (f)) and C2 membranes (*E. coli* (g) and *S. Aureus* (h)) for a period of 2 days.

The results of leaching tests for these blended membranes were depicted in Fig. 8a. In first 24 h, the content of leached zinc ions (0.285 mg L^{-1}) from ZnO NPs/PSF membranes was much higher than the other membranes. Despite the better antibacterial performance achieved, the stability of ZnO nanoparticles in blended membranes is unsatisfactory. On the contrary, core-shell ZnO microspheres exhibited a lower release of Zn^{2+} compared to single-shell ZnO microspheres and nanoparticles, The total concentration of released zinc ions leached from C1 membranes was only 0.221 mg L^{-1}, three times and two times lower than Z membranes and S membranes, respectively. The results indicate that core-shell ZnO microspheres were much more stable than nanoparticles, single-shell microspheres. The reason can be attributed to that a diffusion barrier was created by the shell of ZnO hollow microspheres, which would induce a reduction in the initial burst release form the microspheres [38,39]. Furthermore, the C2 membranes exhibited a lower leakage (0.189 mg L^{-1}) in static systems, only 0.032 mg L^{-1} zinc ions was decreased compared to C1 membrane. Based

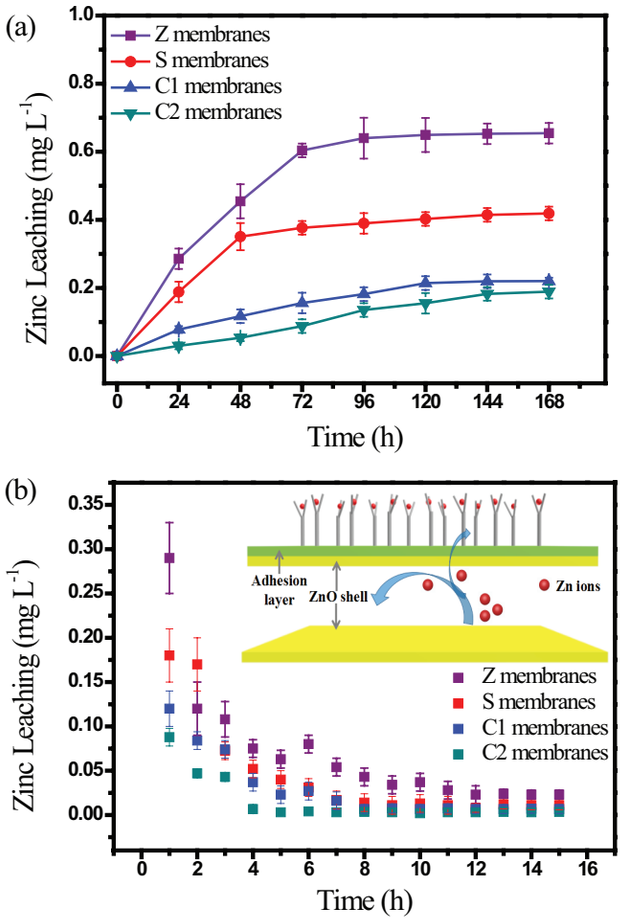

Fig. 8. The loss rate of zinc ions from membranes in immersion test (a); the content of released zinc ions in the filtration experiments (b). Schematic showing the way of release for zinc ions (inset graph). Layers are: yellow/inner shell, dark yellow/outer shell and green/ adhesion layer.

on the experimental results, it implies that majority of generated zinc ions was restricted due to the shell and a small amount of metal ions released from the outer shell was fixed firmly through the functional groups on the surface of adhesion layer (inset graph). It also implied that the design of novel membrane taking advantage of core-shell ZnO microspheres can be more efficient in mitigating the leaching of metal ions than the simple combination of antibacterial nanomaterials and polymer colloids. Fig. 8b depicts the leakage of zinc ions from the blended membranes during 15 h filtration process. According to the world health organization (WHO) guideline, the highest content of zinc ions in drinking water is 1.0 mg/L, three times larger than the initial release of Z membranes (0.290 mg L^{-1}). The leaching of zinc ions occupied 7.25%, 4.11%, 2.19% and 1.86% of the total zinc for Z, S, C1 and C2 membranes, respectively. The results indicate that the release of zinc ions as well as the antibacterial activity of blended membranes can be extended for longer time.

To further assess sustained release property of blended membranes, we took an experiment to verify it, the viability toward *E. coli* was investigated for a period of 4 days. The SEM images for the *E. coli* adhered on the surface of synthesized membrane samples taken away from shaking incubator at each immersion time were exhibited in Fig. 9. In first 4 h immersion, a large mounts of bacteria can be observed on pure PSF and C1 membranes, this can be attributed to the strong attractive electrical interaction force of the samples and *E. coli*, consequently more bacteria were adhered on the surface of these membranes [40]. On the contrary, hardly any bacteria were found to attach on the surface of Z and C2 membranes, which was due to the rapid release of zinc ions in initial stage and the increment of hydrophilicity, respectively. After 24 h immersion, considerable bacteria were still adhered on the surface of pure PSF membrane; however, much less bacteria were attached to C membranes. Despite large qualities of bacteria adhered on the blended membranes in first 4 h, majorities of bacteria were killed by the zinc ions released from the membranes after 24 h. Moreover, it is worth to note that although a mass of bacteria were killed on Z membranes in initial stage, more and more bacteria adhered and grew densely on the Z membranes due to few release of zinc ions after 3 days. Significantly, C membranes still appeared very clean after 4 days immersion, which is consistent with the early discussions that membranes with sustained release property can exhibit long-term anti-biofouling duration.

4. Conclusions

Novel antibacterial and pressure resistant hybrid polysulfone ultrafiltration membranes were successfully fabricated via phase inversion method through employing different kinds of ZnO microspheres as multi-layer nanofillers. The elite multi-layer structure with core-shell microsphere and adhesive levodopa surface were found to exhibit remarkable antimicrobial activity toward *S. aureus* and *E. coli*. Various techniques such as XRD, TEM, FTIR, SEM, contact angle goniometry, uniaxial tension test, antimicrobial and filtration experiments were applied to characterize and investigate the performance of novel membranes. As the rate of zinc ions diffusion can be effectively controlled by the barriers created by the shell of hollow microspheres and the adhesion layer with catechol and indole functional groups, the prepared membranes revealed excellent stability for long-lasting manipulation with little release of zinc ions, in which the leaching rates of C membranes were at least three times and two times lower than that of Z membrane and S membrane, respectively. The pure water flux of prepared membranes with the triple layer structure of core-shell microsphere and levodopa surface were enhanced at least four times higher than that of pure PSF membrane, while the rejection rate for BSA was above 91%. Moreover, the mechanical strength and compatibility of membranes can be greatly enhanced in the meantime due to the multi-shell structure of hollow microspheres and large number of functional groups, which promoted blended membranes to achieve attractive pressure resistant ability as high as 4.63MPa. All these results indicate that novel membranes with multi-shell structure and composition can act as promising candidates for future application in vast fields of chemical separation, food, biomedical and environmental engineering.

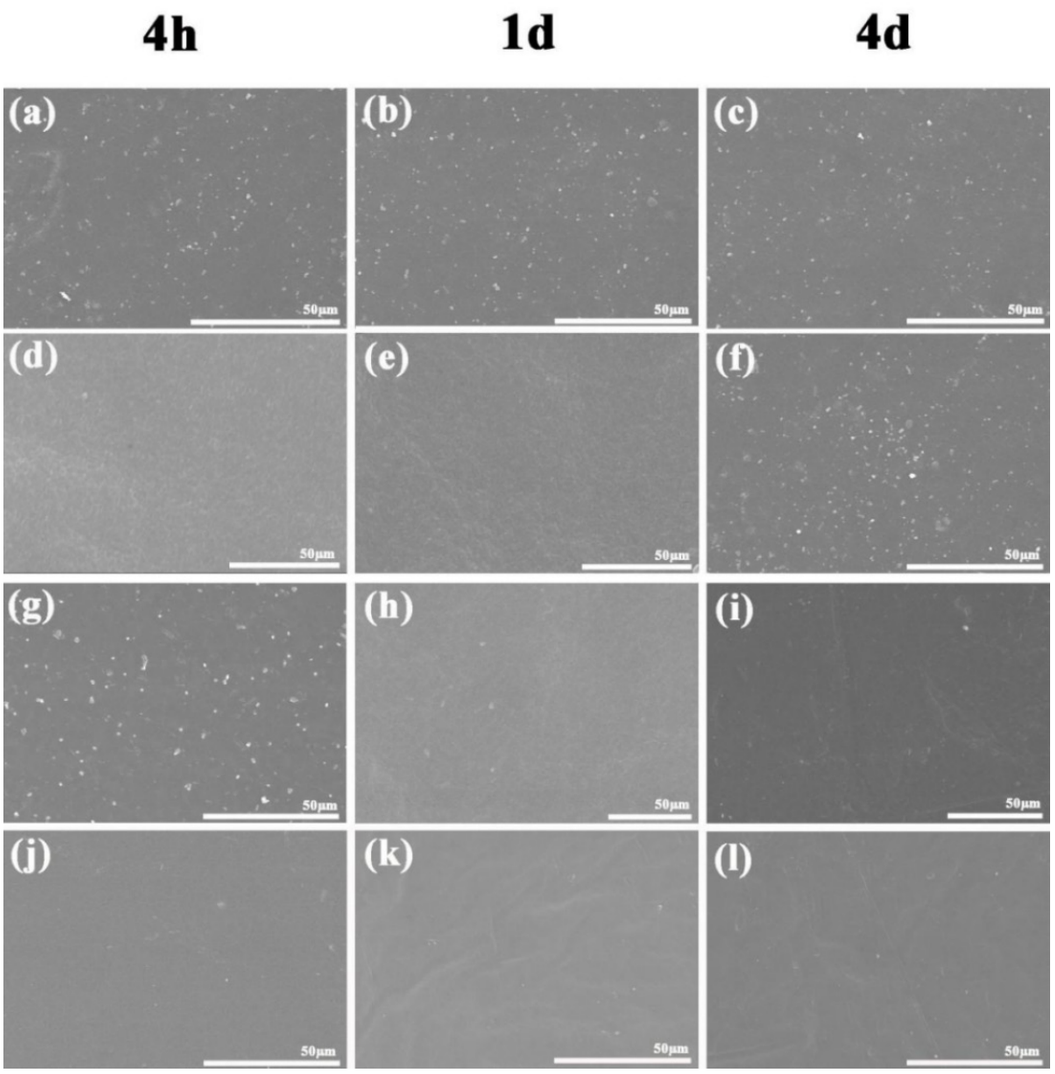

Fig. 9. *E. coli* adhesion and growth on the pure PSF (a, b, c), Z membranes (d, e, f), C1 membranes (g, h, i) and C2 membranes (j, k, l) for a period of 4 days.

Acknowledgements

This work was supported by the National Natural Science Foundation of China (Grant Nos. 21736009, 21236008 and 21476206), Fujian Provincial Department of Ocean (Grant No.2014-06) and Taishan Scholarship Blue Industry Program from Shandong Provincial Government (Grant No. 2014008). G.Z. specially thanks Fujian Provincial Government for the Minjiang Scholarship.

References

[1] N. Abdullah, R.J. Gohari, N. Yusof, A.F. Ismail, J. Juhana, W.J. Lau, T. Matsuura, Polysulfone/hydrous ferric oxide ultrafiltration mixed matrix membrane: Preparation, characterization and its adsorptive removal of lead (II) from aqueous solution, Chem. Eng. J., 289 (2016) 28–37.

[2] C. Shen, Q. Meng, G. Zhang, Chemical modification of polysulfone membrane by polyethylene glycol for resisting drug adsorption and self-assembly of hepatocytes, J. Membr. Sci., 369 (2011) 474–481.

[3] G. Zhang, S.F. Lu, L. Zhang, Q. Meng, C. Shen, J.W. Zhang, Novel polysulfone hybrid ultrafiltration membrane prepared with TiO_2-g-HEMA and its anti-fouling characteristics, J. Membr. Sci., 436 (2013) 163–173.

[4] M.S. Jyothi, V. Nayak, M. Padaki, R.G. Balakrishna, K. Soontarapa, Aminated polysulfone/TiO_2 composite membranes for an effective removal of Cr(VI), Chem. Eng. J., 283 (2016) 1494–1505.

[5] C. Dizman, D.O. Demirkol, S. Ates, L. Torun, S. Sakarya, S. Timur, Y. Yagci, Photochemically prepared polysulfone/poly(ethylene glycol) amphiphilic networks and their biomolecule adsorption properties, Colloids Surf. B: Biointerface, 88 (2011) 265–270.

[6] X. Lin, M. Yang, H. Jeong, M. Chang, J. Hong, Durable superhydrophilic coatings formed for anti-biofouling and oil-water separation, J. Membr. Sci., 506 (2016) 22–30.

[7] Z. Xu, S. Ye, G. Zhang, W. Li, C. Gao, C. Shen, Q. Meng, Antimicrobial polysulfone blended ultrafiltration membranes prepared with Ag/Cu_2O hybrid nanowires, J. Membr. Sci., 509 (2016) 83–93.
[8] Y.F. Zhao, L.P. Zhu, J.H. Jiang, Z. Yi, B.K. Zhu, Y. Xu, Enhancing the antifouling and antimicrobial properties of poly (ether sulfone) membranes by surface quaternization from a reactive poly (ether sulfone) based copolymer additive, Ind. Eng. Chem. Res., 53 (2014) 13952–13962.
[9] R. Goei, T.T. Lim, Ag-decorated TiO_2 photocatalytic membrane with hierarchical architecture: Photocatalytic and antibacterial activities, Water Res., 59 (2014) 207–218.
[10] M.S. Mauter, Y. Wang, K.C. Okemgbo, C.O. Osuji, E.P. Giannelis, M. Elimelech, Antifouling ultrafiltration membranes via post-fabrication grafting of biocidal nanomaterials, ACS Appl. Mater. Interfaces, 3 (2011) 2861–2868.
[11] S. Noimark, J. Weiner, N. Noor, E. Allan, C.K. Williams, M.S.P. Shaffer, I.P. Parkin, Dual-mechanism antimicrobial polymer-ZnO nanoparticle and crystal violet-encapsulated silicone, Adv. Funct. Mater., 25 (2015) 1363–1373.
[12] Y. Li, W. Zhang, J. Niu, Y. Chen, Mechanism of photogenerated reactive oxygen species and correlation with the antibacterial properties of engineered metal-oxide nanoparticles, ACS Nano, 6 (2012) 5164–5173.
[13] I. Sawada, R. Fachrul, T. Ito, Y. Ohmukai, T. Maruyama, H. Matsuyama, Development of a hydrophilic polymer membrane containing silver nanoparticles with both organic antifouling and antibacterial properties, J. Membr. Sci., 387–388 (2012) 1–6.
[14] Y. Chen, Y. Zhang, H. Zhang, J. Liu, C. Song, Biofouling control of halloysite nanotubes-decorated polyethersulfone ultrafiltration membrane modified with chitosan-silver nanoparticles, Chem. Eng. J., 228 (2013) 12–20.
[15] E. Hoseinzadeh, M.Y. Alikhani, M.R. Samarghandi, M. Shirzad-Siboni, Antimicrobial potential of synthesized zinc oxide nanoparticles against gram positive and gram negative bacteria, Desalin. Water Treat., 52 (2014) 4969–4976.
[16] K.R. Raghupathi, R.T. Koodali, A.C. Manna, Size-dependent bacterial growth inhibition and mechanism of antibacterial activity of zinc oxide nanoparticles, Langmuir, 27 (2011) 4020–4028.
[17] Y. Liu, L. He, A. Mustapha, H. Li, Z.Q. Hu, M. Lin, Antibacterial activities of zinc oxide nanoparticles against Escherichia coli O157:H7, J. Appl. Microbiol., 107 (2009) 1193–1201.
[18] Y.J. Jo, E.Y. Choi, S.W. Kim, C.K. Kim, Fabrication and characterization of a novel polyethersulfone/aminated polyethersulfone ultrafiltration membrane assembled with zinc oxide nanoparticles, Polymer, 87 (2016) 290–299.
[19] M. Spasova, N. Manolova, N. Markova, I. Rashkov, Superhydrophobic PVDF and PVDF-HFP nanofibrous mats with antibacterial and anti-biofouling properties, Appl. Surf. Sci., 363 (2016) 363–371.
[20] Z. Dong, X. Lai, J.E. Halpert, N. Yang, L. Yi, J. Zhai, D. Wang, Z. Tang, L. Jiang, Accurate control of multishelled ZnO hollow microspheres for dye-sensitized solar cells with high efficiency, Adv. Mater., 24 (2012) 1046–1049.
[21] S. He, W. Zhang, D. Li, P. Li, Y. Zhu, M. Ao, J. Li, Y. Cao, Preparation and characterization of core-shell avermectin microcapsules based on copolymer matrix of silica-glutaraldehyde-chitosan, J. Mater. Chem B, 1 (2013) 1270–1278.
[22] X. Lai, J. Li, B.A. Korgel, Z. Dong, Z. Li, F. Su, J. Du, D. Wang, General synthesis and gas-sensing properties of multiple-shell metal oxide hollow microspheres, Angew. Chem., 123 (2012) 2790–2793.
[23] V. Vatanpour, S.S. Madaeni, L. Rajabi, S. Zinadini, A.A. Derakhshan, Boehmite nanoparticles as a new nanofiller for preparation of antifouling mixed matrix membranes, J. Membr. Sci., 401–402 (2012) 132–143.
[24] K.R. Raghupathi, R.T. Koodali, A.C. Manna, Size-dependent bacterial growth inhibition and mechanism of antibacterial activity of zinc oxide nanoparticles, Langmuir, 27 (2011) 4020–4028.
[25] A. Bhirud, S. Sathaye, R. Waichal, C.J. Park, B. Kale, In situ preparation of N–ZnO/graphene nanocomposites: excellent candidate as a photocatalyst for enhanced solar hydrogen generation and high performance supercapacitor electrode, J. Mater. Chem A, 3 (2015) 17050–17063.
[26] F. Xiao, Construction of highly ordered ZnO-TiO_2 nanotube arrays (ZnO/TNTs) heterostructure for photocatalytic application, ACS Appl. Mater. Interfaces, 4 (2012) 7055–7063.
[27] L. Yu, Y. Zhang, B. Zhang, J. Liu, H. Zhang, C. Song, Preparation and characterization of HPEI-GO/PES ultrafiltration membrane with antifouling and antibacterial properties, J. Membr. Sci., 447 (2013) 452–462.
[28] H. Rabiee, M.H.D.A. Farahani, V. Vatanpour, Preparation and characterization of emulsion poly (vinylchloride) (EPVC)/TiO_2 nanocomposite ultrafiltration membrane, J. Membr. Sci., 472 (2014) 185–193.
[29] Y. Yang, H.X. Zhang, P. Wang, Q.Z. Zheng, J. Li, The influence of nano-sized TiO_2 fillers on the morphologies and properties of PSF UF membrane, J. Membr. Sci., 288 (2007) 231–238.
[30] M. Safarpour, A. Khataee, V. Vatanpour, Preparation of a novel polyvinylidene fluoride (PVDF) ultrafiltration membrane modified with reduced graphene oxide/titanium dioxide (TiO_2) nanocomposite with enhanced hydrophilicity and antifouling properties, Ind. Eng. Chem. Res., 53 (2014) 13370–13382.
[31] C.Y. Lai, A. Groth, S. Gray, M. Duke, Enhanced abrasion resistant PVDF/nanoclay hollow fibre composite membranes for water treatment, J. Membr. Sci., 449 (2014) 146–157.
[32] J.G. Zhang, Z.W. Xu, W. Mai, C.Y. Min, B.M. Zhou, M.J. Shan, Y.L. Li, C.Y. Yang, Z. Wang, X.M. Qian, Improved hydrophilicity, permeability, antifouling and mechanical performance of PVDF composite ultrafiltration membranes tailored by oxidized low dimensional carbon nanomaterials, J. Mater. Chem. A, 1 (2013) 3101–3111.
[33] Y. Liu, S.L. Zhang, G.B. Wang, The preparation of antifouling ultrafiltration membrane by surface grafting zwitterionic polymer onto poly(arylene ether sulfone) containing hydroxyl groups membrane, Desalination, 316 (2013) 127–136.
[34] Y. Zhang, J. Zhao, H. Chu, X. Zhou, Y. Wei, Effect of modified attapulgite addition on the performance of a PVDF ultrafiltration membrane, Desalination, 344 (2014) 71–78.
[35] H.S. Hwang, J. Song, Y. Jung, O.Y. Kweon, H. Song, J. Jang, Electrospun ZnO/TiO_2 composite nanofibers as a bactericidal agent, Chem. Commun., 47 (2011) 9164–9166.
[36] J. Pasquet, Y. Chevalier, J. Pelletier, E. Couval, D. Bouvier, M.A. Bolzingerb, The contribution of zinc ions to the antimicrobial activity of zinc oxide, Colloids Surf. B: Physicochem. Eng. Asp., 457 (2014) 263–274.
[37] V.B. Schwartz, F. Thétiot, S. Ritz, S. Pütz, L. Choritz, A. Lappas, R. Förch, K. Landfester, U. Jonas, Antibacterial surface coatings from zinc oxide nanoparticles embedded in poly (N-isopropylacrylamide) hydrogel surface layers, Adv Func. Mater., 22 (2012) 2376–2386.
[38] Y.S. Pek, P. Pitukmanorom, J.Y. Ying, Sustained release of bupivacaine for post-surgical pain relief using core-shell microspheres, J. Mater. Chem. B, 2 (2014) 8194–8200.
[39] P. Pitukmanorom, T.-H. Yong, J.Y. Ying, Tunable release of proteins with polymer-inorganic nanocomposite microspheres, Adv. Mater., 20 (2008) 3504–3509.
[40] C.X. Liu, D.R. Zhang, Y. He, X.S. Zhao, R. Bai, Modification of membrane surface for anti-biofouling performance: Effect of anti-adhesion and anti-bacteria approaches, J. Membr. Sci., 346 (2010) 121–130.